

It is easy to show that $S_D(t)$ for a pure superconductor also vanishes like $T \ln T$ as T tends to zero. However, it turns out that in the pure limit there is another contribution to the heat current which is not considered in I and a more elaborate discussion is necessary.¹⁰

Finally, we mention that the extension of the present consideration to the high-field type-II superconductor¹¹ is almost evident. In this case the corrected entropy for a vortex line, can be expressed by

$$S_D(t) = \frac{1}{4eT} \frac{(H_{c2} - B)}{\{1.16[2\kappa_2^2(t) - 1] + 1\}} L(t)A(t), \quad (21)$$

where

$$L(t) = \left\{ 1 + \frac{\frac{1}{2}[1 + b/(b^2 - I^2)^{1/2}]\rho_- \psi^{(2)}(\frac{1}{2} + \rho_-) + \frac{1}{2}[1 - b/(b^2 - I^2)^{1/2}]\rho_+ \psi^{(2)}(\frac{1}{2} + \rho_+)}{\frac{1}{2}[1 + b/(b^2 - I^2)^{1/2}]\psi^{(1)}(\frac{1}{2} + \rho_-) + \frac{1}{2}[1 - b/(b^2 - I^2)^{1/2}]\psi^{(1)}(\frac{1}{2} + \rho_+)} \right\},$$

$$A(t) = \frac{M_d}{(M_d + M_p)}, \quad \rho_{\pm} = \frac{1}{2\pi T} [\epsilon_0 + b \pm (b^2 - I^2)^{1/2}], \quad (22)$$

$\epsilon_0 = 2DeH_{c2}(t)$, $b = (3T_{SO})^{-1}$, and $I = \mu H$. Here μ is the Bohr magneton and T_{SO} is the spin-orbit lifetime. $S_D(t)$ given in Eq. (21) also vanishes like T as T tends to zero.

In conclusion I would like to thank C. Caroli for calling my attention to the difficulty associated with S_D and useful correspondences.

¹A. T. Fiory and B. Serin, Phys. Rev. Letters **16**, 308 (1966), and **19**, 227 (1967).

²F. A. Otter, Jr., and P. R. Solomon, Phys. Rev. Letters **16**, 681 (1966); P. R. Solomon and F. A. Otter, Jr., Phys. Rev. **164**, 608 (1967).

³J. Lowell, J. S. Muñoz, and J. Sousa, Phys. Letters **24A**, 376 (1967).

⁴R. P. Huebener, Phys. Letters **24A**, 651 (1967), and **25A**, 588 (1967).

⁵M. J. Stephen, Phys. Rev. Letters **16**, 801 (1966).

⁶C. Caroli and K. Maki, Phys. Rev. **164**, 591 (1967), hereafter referred to as I.

⁷This difficulty was noted by Dr. Serin and by Dr. Vinen (C. Caroli, private communication).

⁸See, for example, V. Ambegaokar and A. Griffin, Phys. Rev. **137**, A1151 (1965).

⁹C. Caroli and M. Cyrot, Physik Kondensierten Materie **4**, 285 (1965).

¹⁰K. Maki, to be published.

¹¹K. Maki, Phys. Rev. **169**, 381 (1968).

EVIDENCE OF BAND CONDUCTION AND CRITICAL SCATTERING IN DILUTE Eu-CHALCOGENIDE ALLOYS

S. von Molnár and T. Kasuya*

IBM Watson Research Center, Yorktown Heights, New York

(Received 31 October 1968)

Resistivity and Hall-effect measurements in $\text{Eu}_{0.95}\text{Gd}_{0.05}\text{S}$ give evidence for the onset of a well defined conduction band with critical scattering coexisting with magnetic impurity states.

The anomalous properties of Eu-chalcogenide alloys, $\text{Eu}_{1-x}\text{R}_x\text{X}$ (where R is a trivalent rare earth and X is one of the following: O, S, Se, Te) have been the subject of considerable experimental and theoretical investigation.^{1,2} Among these, perhaps the most striking are the anomalous

temperature and field dependence of the resistivity.³ In particular, an explanation of the data on single-crystal samples with $x \leq 0.01$ has been given based on a magnetic impurity state (MIS) and conduction by means of hopping. The activation energy for this process is determined by

the *s-f* exchange interaction between impurity electrons and neighboring Eu ions. This energy decreases precipitously near and below T_C due to the magnetic properties of MIS.^{1,4}

It is to be expected, in analogy with the common semiconductors, that as the trivalent rare earth (in this case Gd) concentration is increased, the conduction process will change from hopping to bandlike. For Ge and Si the start of this transition can be characterized by the ratio of the mean distance between impurity sites, R_i ($R_i = N_i^{-1/3}$, where N_i is the number of impurities per cm^3), to the effective Bohr radius of the impurity electron, a_0 . Experiments indicate that the formation of a band begins at $R_i/a_0 \sim 5$.⁵ In contrast to Ge and Si, the impurity state in Eu chalcogenides is restricted primarily to nearest neighbor (nn) sites. An estimate of a_0 can be made, however, by determining the percentage probability of the MIS wave function beyond the nn site.⁴ This yields a value of $a_0 \sim 2.4 \text{ \AA}$.⁶ Since the number of impurities per cm^3 for doped EuS is $1.89 \times 10^{22}x$, this implies that the impurity states start to merge with the conduction band at the critical impurity concentration $x_C \sim 3\%$. It must be noted that this argument has neglected the effects of *s-f* exchange interaction on band formation. Nonetheless, the existence of a relatively well-defined conduction band is to be expected for a 5% Gd concentration.

Measurements were carried out on small single crystals of $\text{Eu}_{0.95}\text{Gd}_{0.05}\text{S}$. These samples were grown in a 2% excess of Eu metal to reduce compensation. It is not established that this procedure has the desired effect but it will be assumed in the discussion which follows that compensation is negligible. Ordinary ac techniques and the usual five-probe configuration

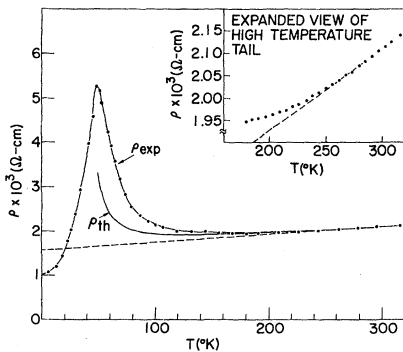


FIG. 1. Temperature dependence of the resistivity ρ in $\text{Eu}_{0.95}\text{Gd}_{0.05}\text{S}$.

were employed.

Figure 1 displays the temperature dependence of the resistivity. Two characteristics of the experimental data are to be noted in particular: (1) The high temperature results indicate a linear dependence of the resistivity on temperature (see insert Fig. 1); (2) the resistivity has a sharp peak at 49°K (the ferromagnetic ordering temperature, T_C , is not well defined in these samples but appears to be a little smaller than the paramagnetic Curie temperature, $\theta \sim 50^\circ\text{K}$). In Fig. 2 are plotted the results of Hall measurements in the paramagnetic region. In magnetic materials the Hall resistivity, e_H , is known to have the general form

$$e_H = R_0 H_i + R_1 M(H_i), \tag{1}$$

where R_0 = normal Hall constant, R_1 = anomalous Hall constant, H_i = internal field, and M = sample magnetization. Furthermore, $H_i = H_a - NM$, where $N = 4.91$ = demagnetization factor for this configuration and H_a is the applied magnetic field. Therefore, with the definition of the susceptibility $M = \chi H_1$, Eq. (1) becomes, in the paramagnetic region,

$$\begin{aligned} \frac{e_H}{H_a} &= R_0 + [R_1 - NR_0] \left\{ \frac{\chi}{1 + N\chi} \right\} \\ &= R_0 + [R_1 - NR_0] \chi^* \end{aligned} \tag{2}$$

As Fig. 2 indicates, a value for $R_0 = -2.85 \times 10^{10} \text{ } \Omega \text{ cm/Oe}$ is found by extrapolation of χ^* to 0. The foregoing analysis implies temperature independence, in the paramagnetic region, of R_0 and R_1 . From the slope of the curve, a value of R_1 may be calculated from the low-field Hall-effect data in the ferromagnetic region. There the analysis follows from Eq. (1), with $e_H/M = R_1$

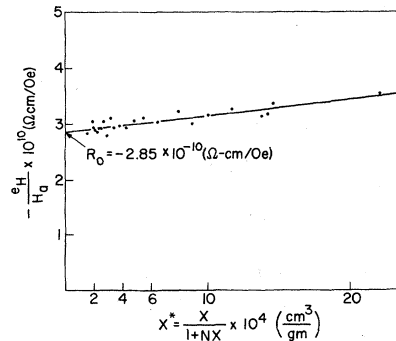


FIG. 2. Slope of curves of Hall resistivity e_H versus applied field H_a in the paramagnetic region, plotted against the effective susceptibility χ^* .

for all values of $H_a < NM_S(T)$ [$M_S(T)$ = saturation moment at temperature T]. Reference is made to Fig. 3, in which is plotted the experimental Hall resistivity as a function of applied magnetic field in both the paramagnetic and ferromagnetic regions. $|R_1|$ increases from 28×10^{10} to 34×10^{10} Ω cm/G in the temperature range from 5 to 30°K.

It should also be noted that the high-field slopes of the 5, 20, and 30°K curves in Fig. 3 are equal, within the experimental error, to the slope at 296°K. Since Eq. (1) may be rewritten as

$$e_H = R_0 H_a + [R_1 - NR_0]M, \quad (3)$$

it is clear that, above saturation, the slope de_H/dH_a is approximately R_0 . Thus, no change in carrier concentration is observed in $\text{Eu}_{0.95}\text{Gd}_{0.05}\text{S}$ throughout the entire temperature range investigated.

The free-electron concentration, $n = 2.2 \times 10^{20}$ cm^{-3} , may be calculated from the well-known formula $R_0 = 10^{-8}/ne$; or $n/N_i \sim 0.24$. This implies that only 24% of the excess electrons occupy the conduction band whereas under the assumption of negligible compensation the other 76% remain in MIS. This conclusion is reasonable in the light of experimental evidence in common semiconductors⁷ which suggests that for concentrations $x_c \leq x < 10x_c$ both localized and band states coexist. Therefore, at $x = 0.05$, the conduction band is only beginning to form. Since the bottom of the conduction band is expected to have s character at the Γ point,¹ the effective-mass approximation will be used with the effective mass m^* equal to the free-electron mass m_0 . A simple calculation then leads to k_F (the Fermi wave vector) = 1.8×10^7 cm^{-1} and E_F (the

Fermi energy) = 0.13 eV. Thus below room temperature the system may be treated as a degenerate Fermi gas.

Since the exchange interaction I_{sf} is estimated to be 0.04 eV,⁴ the exchange splitting, $2I_{sf}S = 0.28$ eV, is larger than $E_F^{\text{ferro}} = 0.21$ eV. In the ferromagnetic state, therefore, all free electrons lie in the spin-up band. These considerations do not, of course, affect the interpretation of the normal Hall-effect measurements which depend only on the number of electrons.

The assumed s character of the conduction band is also consistent with the relatively small value of R_1 . Although the microscopic mechanisms giving rise to R_1 are still a subject of active debate, it is established that the interaction should occur through the orbital angular momentum of the conduction electron which, in an s band, is proportional to k^2 for small values of k . Note that in ferrites, with similar conduction-electron concentration in a d band, R_1 is two orders of magnitude larger.⁸ The notion of the coexistence of conduction electrons and MIS is supported by the fact that the change in paramagnetic Curie temperature from pure EuS ($\theta = 16^\circ\text{K}$) is $\Delta\theta_{\text{exp}} = 34^\circ\text{K}$ in contrast with a rise of, at most, 10°K predicted theoretically⁹ for the effect from conduction electrons alone.

The resistivity ρ may be written as the sum of the residual term ρ_i , the phonon term ρ_p , and the magnetic scattering term ρ_m . Among several types of scattering centers the most significant contribution to ρ_i comes from neutral Gd impurities. With a knowledge of a_0 the scattering potential is evaluated and ρ_i in the ferromagnetic state is obtained, i.e.,

$$\rho_i^f = 1.4(m^*/m_0)^2(5/\epsilon)^2 \times 10^{-3} \Omega \text{ cm}, \quad (4)$$

where ϵ is the effective dielectric constant for the scattering process and should take on a value bracketed by the optical and static dielectric constants, ϵ_0 and ϵ_s , respectively. For pure EuS one finds¹⁰ $\epsilon_0 = 5$ and $\epsilon_s = 11$. The experimental value, $\rho_i^f = 1 \times 10^{-3}$ Ω cm (see Fig. 1), compares favorably with Eq. (4). The same calculation applies to the paramagnetic region and yields $\rho_i^f/\rho_i^p = 0.94$. Therefore ρ_i makes an almost constant contribution to the resistivity over the entire experimental range.

In principle the contribution to phonon scattering in the high-temperature region may come from two sources, acoustic phonons, ρ_p^A , and longitudinal optical phonons, ρ_p^{LO} . The former

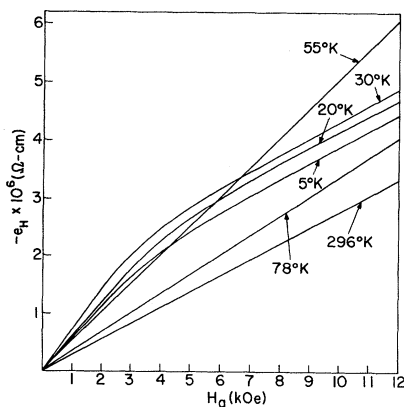


FIG. 3. Field dependence of the Hall resistivity e_H for various temperatures.

(except for relatively low temperatures) leads to the well-known linear dependence on T ,

$$\rho_p^A = 0.2 \left(\frac{m^*}{m_0} \right)^2 \left(\frac{D}{100k\Theta} \right)^2 \frac{T}{100} \times 10^{-4} \Omega \text{ cm},$$

where D is the electron-phonon coupling constant and Θ the Debye temperature ($\Theta_{\text{EuS}} = 208^\circ\text{K}$ ¹¹). The insert in Fig. 1 exhibits the experimental results and confirms acoustic phonon scattering to be the relevant mechanism. The contribution of optical phonons is apparently well screened by the conduction electrons. An estimate of ρ_p^A may be made by extrapolating the high-temperature linear dependence to 0°K (as indicated by the dashed curve in Fig. 1). The result is $\rho_p^A \sim 0.56 \times 10^{-3} \Omega \text{ cm}$ at 300°K , which yields a reasonable value for the electron-phonon interaction, $D \sim 5.5 \text{ eV}$.

The foregoing analysis leaves a magnetic contribution to the resistivity, ρ_m , which is constant down to approximately 200°K , then rises, peaks near T_C , and drops to 0 at 0°K . Such a temperature dependence was first predicted by de Gennes and Friedel¹² who suggested that critical scattering of the conduction electrons ought to occur near T_C . The experimental value of ρ_m at room temperature is $0.56 \times 10^{-3} \Omega \text{ cm}$ corresponds to the spin-disorder scattering resistivity without correlations among the $4f$ spins.¹³ Substitution of $I_{sf} = 0.04 \text{ eV}$, $S = \frac{7}{2}$, $m^* = m_0$ leads to $\rho_m = 0.24 \times 10^{-3} \Omega \text{ cm}$. Agreement is satisfactory. As the temperature decreases to T_C , the correlation between neighboring spins increases and the probability of a correlated giant spin moment increases. The scattering of long-wavelength electrons due to these giant spin moments is the origin of the peak of the resistivity near T_C . In the doped sample, however, there exists another kind of giant spin moment due to MIS and in the 5% sample the larger fraction of the Eu spins contribute to MIS. These two types of giant spin moments enhance each other and, therefore, enhance critical scattering. The long, sizable tail of the magnetic specific heat of doped EuS appears to be due to this phenomenon.¹⁴ A realistic calculation of the correlation function γ is, therefore, very complicated. Figure 1 exhibits the calculated results for ρ_m based on a γ derived for a simple nearest-neighbor ferromagnet. This γ should be correct for pure EuO and EuS and, in fact, fits the experimental specific-heat data. The discrepancy between theory and experiment, particularly at relatively high temperatures, is apparently due to MIS.

It is interesting to note that critical scattering appears not to be observed in CdCr_2Se_4 .¹⁵ The authors hereof suggest that, in CdCr_2Se_4 , the s - d exchange interaction is much larger than the s - f interaction and consequently the simple Born approximation is not applicable.¹⁶ Under these circumstances magnetic polaron effects would seem to be important.

This paper has presented evidence for band conduction and critical scattering in $\text{Eu}_{0.95}\text{Gd}_{0.05}\text{S}$. Magnetic impurity states are believed to coexist with conduction electrons in this concentration range. This is consistent with the impurity hopping model applicable for very low concentrations. In this connection, it should be noted that magnetic semiconductors may prove to be more useful than the usual nonmagnetic semiconductor for the study of the general character of impurity states. This is a consequence of the additional information gained through the s - f interaction.

The authors would like to thank Dr. M. W. Shafer for kindly providing samples, Dr. T. R. McGuire for performing magnetic measurements, Dr. T. D. Schultz and Dr. S. Methfessel for many valuable discussions, and E. Battista for his able assistance.

*Permanent address: Department of Physics, Tohoku University, Sendai, Japan.

¹T. Kasuya and A. Yanase, to be published.

²S. Methfessel and D. C. Mattis, *Handbuch der Physik* (Springer-Verlag, Berlin, Germany, 1968), Vol. 18, Pt. 1; also see introduction of Ref. 1.

³J. C. Suits, *Bull. Am. Phys. Soc.* **8**, 381 (1963); R. R. Heikes and C. W. Chen, *Physics* **1**, 159 (1964); S. von Molnár and S. Methfessel, *J. Appl. Phys.* **38**, 959 (1967).

⁴A. Yanase and T. Kasuya, to be published.

⁵H. Fritzsche, *J. Phys. Chem. Solids* **6**, 69 (1958); also see C. Yamanouchi, K. Miziguchi, and W. Sasaki, *J. Phys. Soc. Japan* **22**, 859 (1967).

⁶T. Kasuya and A. Yanase, to be published. This estimate, although made for EuSe, is not expected to differ substantially for EuS.

⁷C. Yamanouchi and W. Sasaki, private communication; S. Maekawa, *J. Phys. Soc. Japan Suppl.* **21**, 574 (1966).

⁸J. M. Levine, *Phys. Rev.* **114**, 482 (1959); A. A. Samokhvalov and A. G. Rustamov, *Fiz. Tverd. Tela* **7**, 1198 (1965) [translation: *Soviet Phys.—Solid State* **7**, 961 (1965)].

⁹T. Kasuya, in *Magnetism*, edited by G. T. Rado and H. Suhl (Academic Press, Inc., New York, 1966) Vol. IIB. The method of calculation is the same as for the rare-earth metals.

¹⁰J. Axe, private communication.

¹¹V. L. Moruzzi and D. T. Teaney, *Solid State Commun.* **1**, 127 (1963).

¹²P. G. de Gennes and T. Friedel, *J. Phys. Chem. Solids* **4**, 71 (1958).

¹³T. Kasuya, *Progr. Theoret. Phys. (Kyoto)* **16**, 58 (1956).

¹⁴V. L. Moruzzi, D. T. Teaney, and B. J. C. van der Hoeven, Jr., *Solid State Commun.* **6**, 461 (1968).

¹⁵C. Haas, A. M. J. G. Van Run, P. F. Bongers, and W. Albers, *Solid State Commun.* **5**, 657 (1967); H. W. Lehmann, *Phys. Rev.* **163**, 488 (1967); C. Haas, *ibid.* **168**, 531 (1968).

¹⁶The details will be treated in another paper.

DETECTION OF ELECTRIC-FIELD TURBULENCE IN THE EARTH'S BOW SHOCK*

R. W. Fredricks, C. F. Kennel,† F. L. Scarf, G. M. Crook, and I. M. Green
Space Sciences Laboratory, TRW Systems Group, Redondo Beach, California 90278
(Received 28 October 1968)

We present the first account of observation of low-frequency fluctuating electric fields generated in the earth's bow shock. We find that the wave amplitude is not a smooth function of space through the shock, but rather that it is strongly correlated with magnetic-field structures within the shock.

OGO-5 was launched 4 March 1968 into a highly eccentric earth orbit with an apogee of 24 earth radii ($\approx 148\,000$ km) geocentric. The TRW plasma-wave experiment on board OGO-5 includes five electric-dipole and three magnetic-loop (search coil) sensors mounted on a 22-ft boom. Three short electric-dipole sensors are mounted orthogonally, so that all three electric-field vector components can be measured in time sequence. The output is fed into narrow-band (15%) filters with center frequencies at 0.56, 1.3, 3.0, 7.35, 14.5, 30.0, and 70.0 kHz. The circuits have rise times of 30 msec and decay times of 300 msec. In a given frequency band, each directional component is sampled for 9.2 sec sequentially; after 27.6 sec the center frequency is advanced to the next channel. A complete axis and frequency scan sequence requires 3.2 min. In addition, the wave form on one axis is continuously monitored by a separate broadband (1-22 kHz) analog telemetry system, permitting reconstruction of the power spectrum for this one axis. The remaining two boom-mounted dipoles are collinear. Their output is monitored through a 200-Hz center-frequency filter for about 2 sec every 9.2 sec. The five electric dipoles do not operate as resistively coupled Langmuir probes, but rather are capacitively coupled to the plasma¹ since the dipole dimensions (50 cm) are much smaller than the Debye length, and the current collecting area is small. The dipoles measure potential gradients induced across them by ambient electric fields. The three electrostatically shielded magnetic loops are boom-

mounted orthogonal to the main electric dipoles, and they are sequentially sampled by axis and by frequency through 0.56- and 70-kHz filters. The 0.56-kHz magnetic output is phase-shifted, mixed with the 0.56-kHz electric output, and monitored through a zero-crossing correlator, so that electrostatic and electromagnetic waves may be separated.

Figure 1 presents a sequence of approximate electric-field power spectra assembled from the band-pass channel outputs for an outbound shock crossing on 12 March 1968. The abscissa is the frequency from 0.56 to 70 kHz; the ordinate, the maximum power spectral density (regardless of axis) in $(\mu\text{V}/\text{m})^2/\text{Hz}$ observed in each 27.6-sec channel sample. The time axis is orthogonal to these two, and is shown in perspective along the 45° axis. Each spectrum requires 3.2 min; the initiation of a new spectral sequence is indicated by tick marks along the time axis. Near the origin, OGO-5 was downstream in the post-shock magnetosheath; as time proceeded, the outbound satellite traversed the shock. At the top of Fig. 1, OGO-5 was upstream. Shown in small insets are simultaneous measurements of one component of the magnetic field detected by the University of California at Los Angeles (UCLA) flux-gate magnetometer (sensitive from 0-2.5 Hz at the 8-kbit/sec rate). Upstream (top of Fig. 1) in the solar wind, the magnetic field is quiet, and the electric-field spectrum contains a significant high-frequency component (indicated by shading) which may be near the local electron plasma frequency. Nearer the shock, where the magnetic